Elastic Scattering and Reactions of Protons on O^{18}†

R. R. CARLSON, C. C. KIM,* J. A. JACOBS,‡ AND A. C. L. BARNARD§
Department of Physics and Astronomy, State University of Iowa, Iowa City, Iowa
(Received December 14, 1960)

The elastic scattering $O^{18}(p,p)O^{18}$ and the reactions $O^{18}(p,p'\gamma)O^{18}$, $O^{18}(p,\alpha_0)N^{15}$, and $O^{18}(p,\alpha_{1,2}\gamma_{1,2})N^{15}$ were studied using a thin gas target with the State University of Iowa electrostatic generator. Absolute differential cross sections were measured for the two laboratory angles 86.8° and 159.5° in the incident proton energy range 790 to 3550 kev and angular distributions for α_0 and p were measured at several energies. Relative yield curves of gamma rays were obtained in the same energy range as above. Two F^{19} levels were observed which have not been previously reported and some new decay modes for previously known levels were observed. From consideration of the detailed shape of the elastic-scattering anomalies and the angular distributions, spin and parity assignments were made to some F^{19} levels.

INTRODUCTION

PROTON capture by an O^{18} nucleus forms an F^{19} compound nucleus with excitation energy 7.964 Mev[1] plus the kinetic energy in the center-of-mass system. Studies of the elastic scattering of such protons and their reactions as a function of proton energy, and of the angular distributions of the outgoing particles, can provide information about the existence, spin, and parity of energy levels in the compound nucleus. A number of energy levels in F^{19} have been found from studies of the $O^{18}(p,\alpha_0)N^{15}$ reaction[2–6] and levels have also been found from the yield of gamma rays[2,7,8] and neutrons.[9–11] Figure 1 shows energy levels of the nuclei involved in the interaction of protons and O^{18}.

Theoretically the F^{19} nucleus has been successfully treated, using configuration mixing in an intermediate-coupling shell model, by Elliot and Flowers[12] and by Redlich.[13] Paul[14] has applied a rotational model with some success and recently Sheline and Wildermuth[15] have made predictions on the basis of a cluster model.

In the present work absolute differential cross sections for proton elastic scattering and for the following reactions:

$O^{18}(p,p')O^{18*}$ (1.982-Mev first excited state)
$O^{18}(p,\alpha_0)N^{15}$ (ground state)
$O^{18}(p,\alpha_{1,2})N^{15*}$ (5.28-Mev and/or 5.31-Mev states)

were studied by observing charged particles at laboratory angles 86.8° and 159.5° in the range of incident proton energies $790<E_p<3550$ kev. Gamma-ray yield curves at 90° were also obtained. Angular distributions of elastically-scattered protons and α_0 particles were measured at several resonances. A number of levels were observed in addition to those found by previous workers in the same energy range.

An attempt was made to analyze the elastic scattering data and the (p,α_0) data using an approximate form of the dispersion theory.[16] Even at the lower bombarding

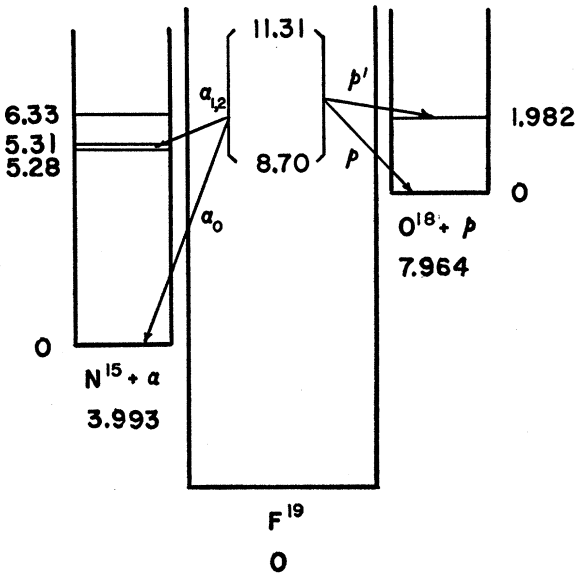

FIG. 1. Energy level diagram. Energies are given in Mev.

† Supported in part by the U. S. Atomic Energy Commission.
* Now at Physics Department, University of Southern California, Los Angeles, California.
‡ Now at Physics Department, Virginia Polytechnic Institute, Blacksburg, Virginia.
§ Now at Physics Department, Rice University, Houston, Texas.
[1] F. Ajzenberg-Selove and T. Lauritsen, Nuclear Phys. **11**, 255 (1959).
[2] H. A. Hill and J. M. Blair, Phys. Rev. **104**, 198 (1956); J. M. Blair and J. J. Leigh, Phys. Rev. **118**, 495 (1960).
[3] R. L. Clarke, E. Almquist, and E. B. Paul, Nuclear Phys. **14**, 472 (1959).
[4] J. Seed, Phil. Mag. **42**, 566 (1951).
[5] C. Mileikowsky and R. T. Pauli, Arkiv Fysik **4**, 299 (1950).
[6] A. V. Cohen, Phil. Mag. **44**, 583 (1953).
[7] J. W. Butler and H. D. Holmgren, Phys. Rev. **99**, 1649 (1955).
[8] E. L. Hudspeth, I. L. Morgan, and J. T. Peoples, Phys. Rev. **99**, 643 (1955); J. W. Nelson and E. L. Hudspeth, Bull. Am. Phys. Soc. **5**, 109 (1960), and private communication.
[9] H. T. Richards, R. V. Smith, and C. P. Browne, Phys. Rev. **80**, 524 (1950).
[10] J. P. Blaser, F. Boehm, P. Marmier, and P. Scherrer, Helv. Phys. Acta **24**, 465 (1951).
[11] H. Mark and C. Goodman, Phys. Rev. **101**, 768 (1956).
[12] J. P. Elliot and B. H. Flowers, Proc. Roy. Soc. (London) **A229**, 536 (1955).
[13] M. G. Redlich, Phys. Rev. **99**, 1427 (1955).
[14] E. B. Paul, Phil. Mag. **2**, 311 (1957).
[15] R. K. Sheline and K. Wildermuth, Bull. Am. Phys. Soc. **5**, 271 (1960).
[16] R. G. Sachs, *Nuclear Theory* (Addison-Wesley Publishing Company, Reading, Massachussetts, 1953).

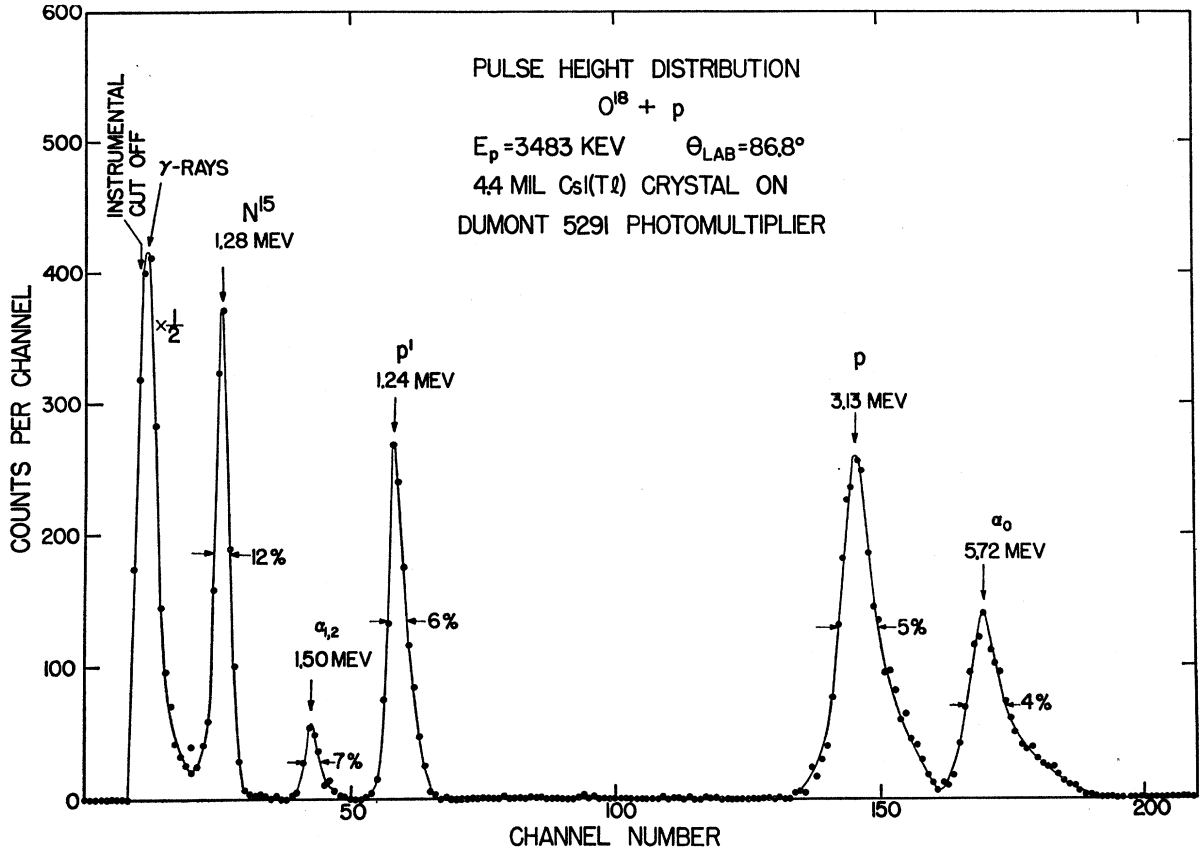

FIG. 2. Pulse-height spectrum from the charged-particle detector at $E_P = 3483$ kev. At lower incident energies the p' and $\alpha_{1,2}$ peaks are absent.

energies this requires consideration of interference between levels. The analysis was consequently limited to the more prominent anomalies.

EXPERIMENTAL METHOD

Apparatus

A proton beam from the State University of Iowa electrostatic generator passed through a 1000 A thick nickel foil into the target gas. After traversing the gas, the beam left the chamber through a 3750 A thick nickel foil and entered a vacuum Faraday cup. Reaction products and scattered protons originating in a well-defined reaction volume in the chamber could pass through a defining system into a charged-particle detector [a 0.004-in. thick CsI(Tl) wafer]. This detector was mechanically part of the upper part of the chamber, which could be rotated relative to the fixed lower part. By this means the angle of observation (relative to the incoming beam direction) of charged particles was variable between 20.5° and 159.5°. A gamma-ray detector [2-in. diameter $\times 1\frac{3}{4}$-in. long NaI(Tl) crystal] remained fixed at 90°. Conventional electronic equipment was used in conjunction with the detectors. The temperature and pressure of the target gas were measured with a thermocouple and an octoil manometer. A dry-ice/acetone cold trap was used in the chamber and the temperature of the gas at the reaction volume was about 270°K. Pressures of about 2.5 mm of mercury were used, corresponding to a target 4.5 kev thick to 2-Mev protons. The apparatus has been changed only slightly since it was described in detail by Bashkin, Carlson, and Douglas.[17]

An electrolysis system was used to obtain the target gas from water enriched in O^{18}, the functioning of the electrolysis system being checked by electrolyzing ordinary water and measuring an absolute differential cross section for protons on O^{16}. The cross section obtained in this way differed from that obtained using commercial tank oxygen by less than 0.5%.

The enriched water was obtained from the Weizmann Institute, where analysis gave the oxygen isotopic composition 90.0% O^{18}, 1.2% O^{17}, and 8.8% O^{16}. This rating was checked by mass spectrometer analysis. The O^{18} content was also checked by a comparison of the yield of the (p,α_0) reaction at the 844-kev resonance for targets of the enriched gas and natural oxygen. The checks were in agreement with the suppliers' figures.

[17] S. Bashkin, R. R. Carlson, and R. A. Douglas, Phys. Rev. 114, 1543 (1959).

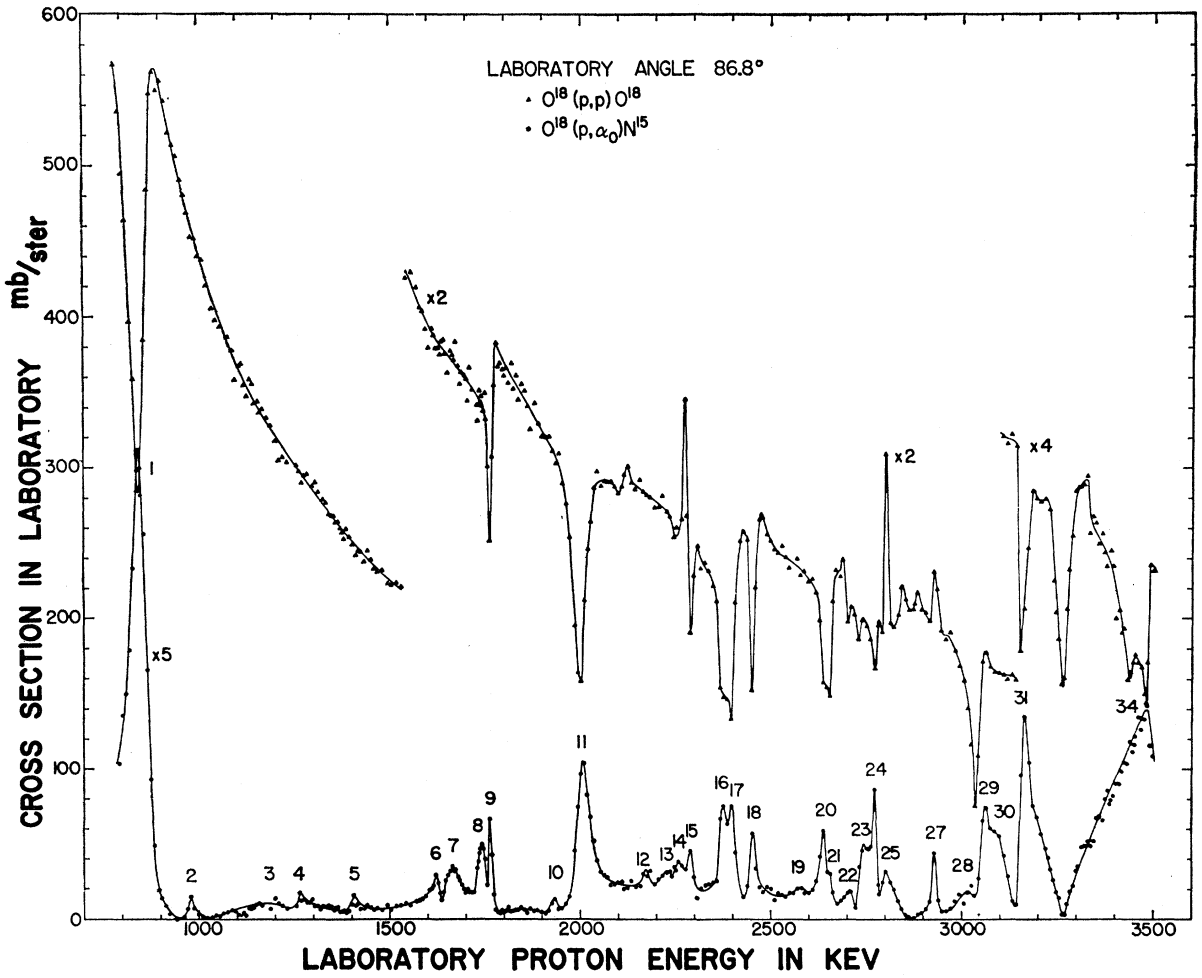

FIG. 3. Absolute laboratory differential cross sections for $O^{18}(p,p)O^{18}$ and $O^{18}(p,\alpha_0)N^{15}$ as a function of laboratory proton energy observed at laboratory angle 86.8°.

The 6-liter gas target chamber was sufficiently free of any material evolving gas that the enriched oxygen gas, at a pressure of a few mm of Hg, could be kept for several days without appreciable contamination. Contamination was checked regularly by running over a resonance for the (p,α_0) reaction at low bombarding energy (844 kev). The maintenance of both the α_0 yield and the yield of elastically scattered protons was used as a guarantee of purity.

Yield Measurements

The pulse-height spectrum from the charged-particle detector at low bombarding energy has three well-defined peaks, corresponding to elastically scattered protons, α_0 particles, and recoil N^{15} ions. In Fig. 2 the spectrum for a higher bombarding energy is shown. Two additional peaks are present, from inelastically scattered protons leaving O^{18} in its first excited state ($E_x=1.982$ Mev) and α particles leaving the residual N^{15} nucleus in its first and/or second excited states ($E_x=5.276$, 5.305 Mev). These groups are denoted by p' and $\alpha_{1,2}$, respectively. A complete pulse-height spectrum was recorded, by printing out from a 256-channel analyzer, at each incident proton energy and, in addition, yields were recorded using four scaling channels responding to pulses above appropriately chosen discriminator levels.

EXPERIMENTAL RESULTS

Absolute Differential Cross Sections for Elastic Scattering and the α_0 Reaction

In Figs. 3 and 4, the laboratory differential cross sections for the elastic scattering $O^{18}(p,p)O^{18}$ and the reaction $O^{18}(p,\alpha_0)N^{15}$ are plotted for the proton bombarding energy range between 790 and 3550 kev for the laboratory angles 86.8° and 159.5°, respectively. Gamma-ray yield curves at 90° were obtained simultaneously and an example appears in Fig. 4. Comparing the yield curves for charged particles and for gamma rays, it is noted that the particle resonances are dis-

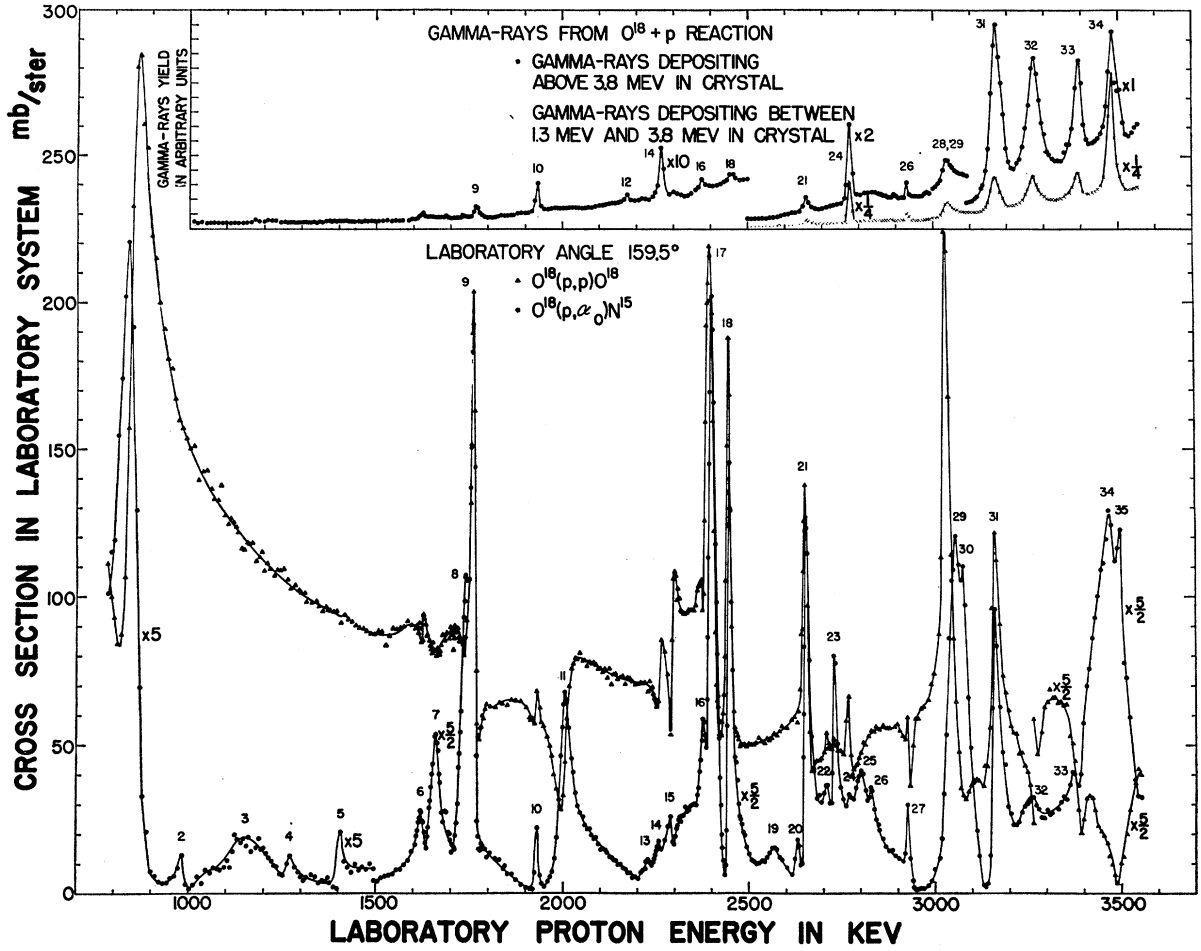

FIG. 4. Absolute laboratory differential cross sections for $O^{18}(p,p)O^{18}$ and $O^{18}(p,\alpha_0)N^{15}$ as a function of laboratory proton energy observed at laboratory angle 159.5°. The gamma-ray yield curve (upper part of figure) was observed at 90°.

placed from those of the gamma rays by a few kev. This is because the center of the reaction volume as seen by the particle detector differs from that seen by the gamma-ray detector. The gamma-ray yield curve also shows less structure than the particle yield curve because the gamma-ray detector has a much thicker effective target.[17] The gamma-ray detector was used mainly as an energy monitor enabling particle yield curves taken at different angles to be lined up in energy.

It was necessary to correct the elastic-scattering data for the elastic scattering due to O^{16} and O^{17}. The elastic scattering for O^{16} was measured over the energy range using ordinary oxygen (99.76% O^{16}). The results agreed with those of other investigators.[18] No data were available on elastic scattering from O^{17}, so accurate corrections could not be made. Since the O^{17} content of the gas used was only 1.2%, no appreciable error should result. The elastic scattering cross section of O^{18} is believed known to $\pm 5\%$ where the increased error over previous measurements[17] with this apparatus occurs because of the above correction for the presence of O^{16}.

In Fig. 5 the angular distributions for $O^{18}(p,p)O^{18}$ and $O^{18}(p,\alpha_0)N^{15}$ are plotted at several resonances.

$O^{18}(p,p')O^{18*}$ and $O^{18}(p,\alpha_{1,2})N^{15*}$ Reactions

The two additional charged-particle groups in the spectra at high incident proton energies were identified as coming from these two reactions, by considering the change in the pulse height of the group with incident proton energy and the change in pulse height with the interposition of absorber. This latter feature (a facility added to the gas target chamber since previous work was done[17]) clearly differentiated alpha particles from protons. In Fig. 6 the differential cross sections for the two reactions are shown. They are believed known to $\pm 8\%$ for these particles as before.[17]

Figure 7 shows the gamma-ray spectrum taken at the 3483-kev resonance. The energies of the two gamma-

[18] F. J. Eppling, J. R. Cameron, R. H. Davis, A. S. Divatia, A. I. Galonsky, E. Goldberg, and R. W. Hill, Phys. Rev. **91**, 438(A) (1953). Also, unpublished data quoted in the Los Alamos Report LA-2014, 1956 (unpublished).

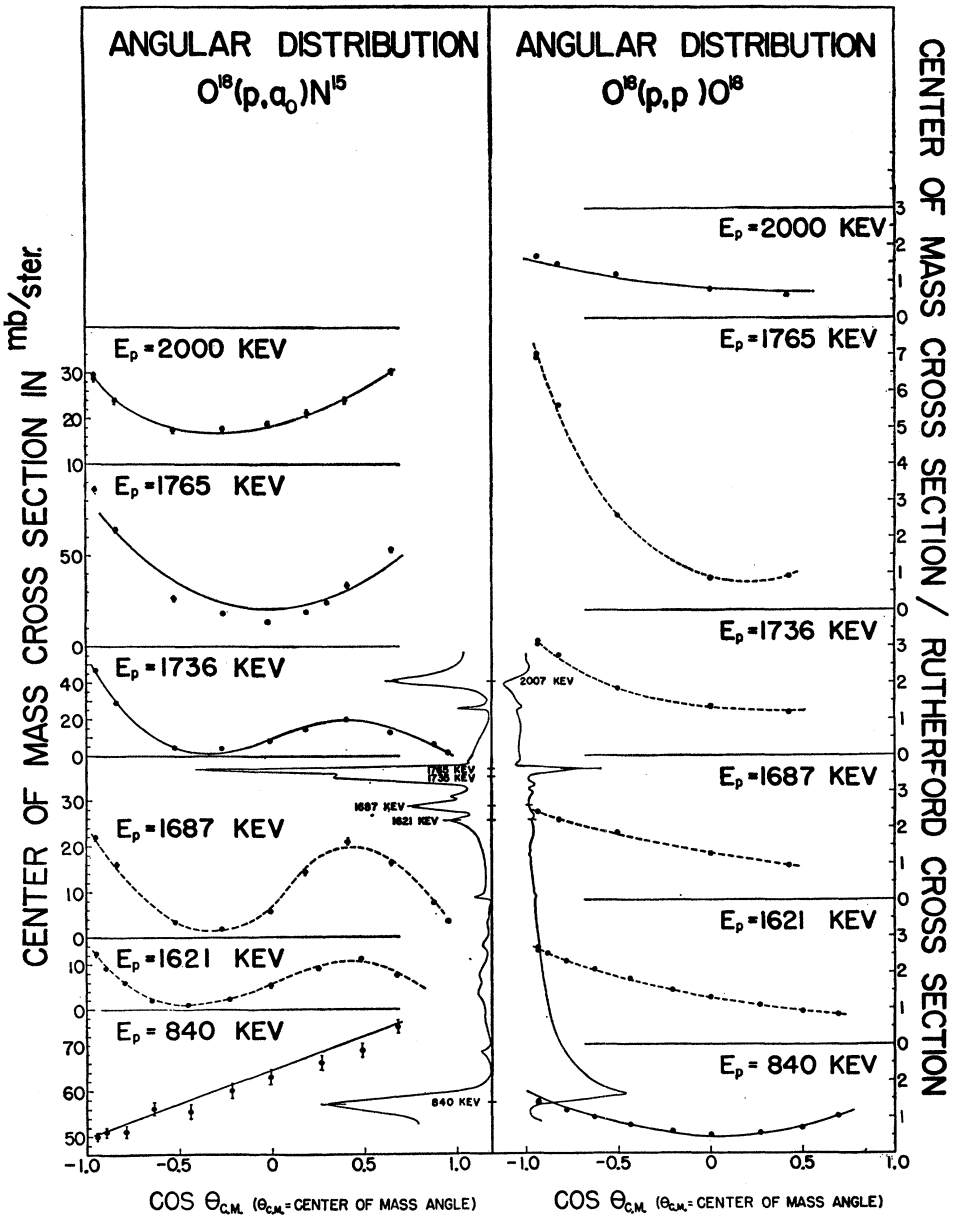

FIG. 5. Angular distributions for $O^{18}(p,p)O^{18}(p,\alpha_0)N^{15}$ measured at several resonances. Solid lines are calculated.

ray groups which appear confirm the identification of the reactions.

ENERGY LEVELS IN F^{19} FROM THE $O^{18}+p$ EXPERIMENT

The target thickness in the present work was 4.5 kev for 2-Mev protons, whereas that in the work by Hill and Blair[2] was 26 kev and that in the work of Clarke *et al.*[3] was about 20 kev. Because of the better energy resolution and the fact that observations were made at 159.5° as well as 86.8°, a number of additional resonances were observed. Table I lists the resonances observed in the present work together with observed decay modes. For resonances which have been observed before there were new decay modes observed and these are included in the list. An asterisk at the resonance number shows those levels which have not previously been observed by any of the decay modes listed. The resonance energies were taken off the 86.8° curve wherever possible.

The following is a brief discussion of some of the resonances:

Resonance 3. This resonance is presumably due to a different level than that observed by Butler and Holmgren[7] in the $O^{18}(p,\gamma)F^{19}$ reaction and assigned $T=\frac{3}{2}$, since its width is much greater here.

TABLE I. Energy levels of F^{19} from $O^{18}(p\alpha_0)N^{15}$, $O^{18}(p,p)O^{18}$, $O^{18}(p,p')O^{18}$, and $O^{18}(p,\alpha_{1,2\gamma 1,2})N^{15}$.

Present work				Hill and Blair[a]		Clarke *et al.*[b]	
Resonance	E_p (kev)	E_x (Mev)	Observed decay modes	Resonance	E_p (kev)	Resonance	E_p (kev)
1	844±6	8.763	p, α_0	1	838	1	838
2	980±6	8.892	α_0	2	980	2	991
3	1160±20	9.062	α_0	...	...	3	1182
4	1271±10	9.168	α_0	3	1271	4	1308
5	1406±6	9.296	α_0	4	1406	5	1390
6	1620±6	9.498	p, α_0	5	1621	6	1639
7	1668±6	9.544	p, α_0	6	1688	7	1676
8	1736±6	9.609	α_0	7	1736	8	1740
9	1765±5	9.636	p, α_0, γ	8	1761	9	1760
...	...	...	...	...	...	10	1870
10	1932±6	9.794	p, α_0, γ	9	1934	11	1941
11	2007±5	9.865	p, α_0	10	2007	12	2006
...	...	...	...	...	...	13	2037
12	2175±7	10.024	α_0, γ	11	2175	...	...
13	2230±7	10.076	α_0	12	2232	...	...
14	2260±7	10.105	p, α_0, γ	13	2258	...	...
15	2291±7	10.135	p, α_0	14	2291	14	2299
16	2378±7	10.217	p, α_0, γ	15	2378	15	2369
17	2403±7	10.240	p, α_0	...	...	16	2389
18	2452±7	10.287	p, α_0, γ	16	2450	17	2450
19*	2570±8	10.398	α_0	...	...	...	...
20	2636±8	10.461	p, α_0	17	2635	18	2631
21*	2648±8	10.472	p, α_0, γ	...	...	...	...
22	2708±8	10.529	p, α_0	18	2712	19	2708
23	2726±8	10.546	p, α_0	...	...	20	2737
24	2768±8	10.586	p, α_0, p'	19	2767	21	2771
25	2800±8	10.617	p, α_0	20	2798	22	2803
26*	2824±8	10.639	p, α_0, p'	...	...	...	...
27	2926±8	10.736	p, α_0	21	2929	23	2922
28	3026±8	10.831	α_0, p'	22	3029	...	...
29	3064±9	10.867	p, α_0, $\alpha_{1,2}$	23	3064	24	3045
30	3080±9	10.881	α_0	...	...	25	3075
31	3165±8	10.962	p, α_0, p', $\alpha_{1,2}$	24	3165		
32*	3266±9	11.058	p, α_0, p', $\alpha_{1,2}$	...	...		
33*	3386±9	11.172	p, α_0, p', $\alpha_{1,2}$	...	...		
34	3480±9	11.261	p, α_0, p', $\alpha_{1,2}$	25	3473		
35*	3502±9	11.282	α_0, $\alpha_{1,2}$				

[a] See reference 2.
[b] See reference 3.

Resonance 19. This level has not been seen before. It appears at both angles of observation although less obviously at 86.8°.

Resonance 21. This level is seen in the (p,n)[2] and (p,γ)[8] yields. It is unresolved here at 90° but is dominant at 159.5°.

Resonance 26. This level may correspond to one seen in the (p,γ) yield.[8] The resonance appears at 159.5° but not at 86.8°.

Resonance 32, 33. These levels are seen in the pn yield. They appear in the $p\alpha_0$ yield at 159.5° but not at 86.8°.

Resonance 35. This level has not been previously reported.

There are two levels previously unobserved—No. 19, No. 35—and four previously unobserved in the (p,α_0) reaction.

DIFFERENTIAL CROSS SECTION IN TERMS OF FUNDAMENTAL PARAMETERS

Analysis of Elastic Scattering

The method of analysis of scattering cross sections for spin-zero target nuclei, such as O^{18}, is well known.[19] In the present case neighboring levels interfere and reactions are possible so that the number of parameters which must be used to fit the elastic scattering cross section in detail can become excessive. For this reason the qualitative behavior of the elastic scattering cross section is particularly important. In the one-level approximation the elastic scattering cross section takes the form:

$$\frac{d\sigma}{d\Omega}=\frac{1}{k^2}\Big|-\tfrac{1}{2}\eta_p\csc^2(\theta/2)\exp[i\eta_p\ln\csc^2(\theta/2)]+\sum_{l=0}^{\infty}(l+1)P_l(\cos\theta)e^{2i\omega_{pl}}\{\sin\psi_{pl}e^{i\psi_{pl}}+a_{pl}{}^{+}\sin\delta_l{}^{+}\exp[i(\delta_l{}^{+}+2\psi_{pl})]\}$$
$$+\sum_{l=1}^{\infty}lP_l(\cos\theta)e^{2i\omega_{pl}}\{\sin\psi_{pl}e^{i\psi_{pl}}+a_p{}^{-}\sin\delta_l{}^{-}\exp[i(\delta_l{}^{-}+2\psi_{pl})]\}\Big|^2+\frac{\sin^2\theta}{k^2}\Big|\sum_{l=1}^{\infty}P_l'(\cos\theta)e^{2i\omega_{pl}}$$
$$\times\{a_{pl}{}^{-}\sin\delta_l{}^{-}\exp[i(\delta_l{}^{-}+2\psi_{pl})]-a_{pl}{}^{+}\sin\delta_l{}^{+}\exp[i(\delta_l{}^{+}+2\psi_{pl})]\}\Big|^2.$$

[19] J. W. Olness, W. Haeberli, and H. W. Lewis, Phys. Rev. **112**, 1702 (1958).

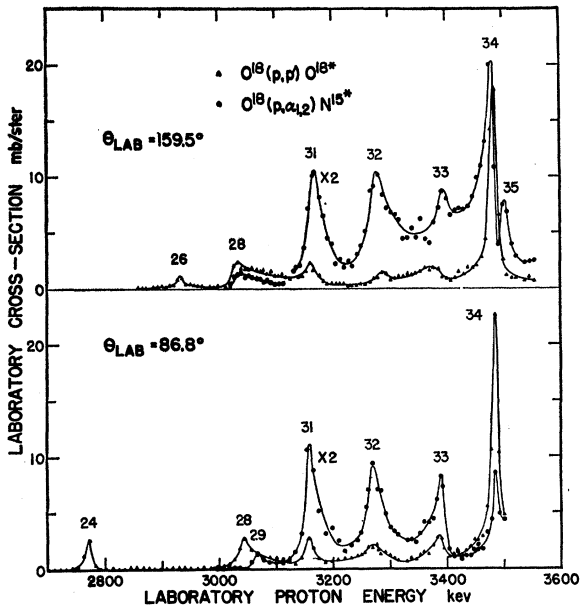

FIG. 6. Absolute cross sections for $O^{18}(p,p')O^{18*}$ and $O^{18}(p,\alpha_{1,2})N^{15*}$ as a function of laboratory proton energy observed at laboratory angles 86.8° and 159.5°.

The first term on the right arises from the Coulomb scattering amplitude and the nuclear scattering coherent with it. The second term on the right arises from scattering with spin flip. Notation is standard; briefly,

$$\omega_{xl}=\sum_{n=1}^{l}\tan^{-1}(\eta_x/n), \quad \omega_{x0}=0,$$

$$\eta_x=Z_1Z_2e^2/\hbar v,$$

where x denotes the pair interacting with p for $O^{18}+p$ and α for $N^{15}+\alpha$. $\delta_l^{\pm}$ is the resonance phase shift for the level formed with $J=l\pm\frac{1}{2}$ and has the value $\tan^{-1}[(\Gamma/2)(E_R-E)^{-1}]$, where Γ is the total width of the resonance level. $a_{xm}^{\pm}$ is the fractional partial width for decay of the level with spin $J=l\pm\frac{1}{2}$ into the pair x with the orbital angular momentum m (in units of $\hbar$). P_l is the Legendre polynomial and P_l' is the derivative of it with respect to $\cos\theta$, θ being the center-of-mass angle of the light outgoing particle. k is the center-of-mass wave number of the bombarding proton and v is its laboratory velocity.

In the present work all of the potential phase shifts, ψ_{pl}, except ψ_{p0} were set equal to zero. Those set equal

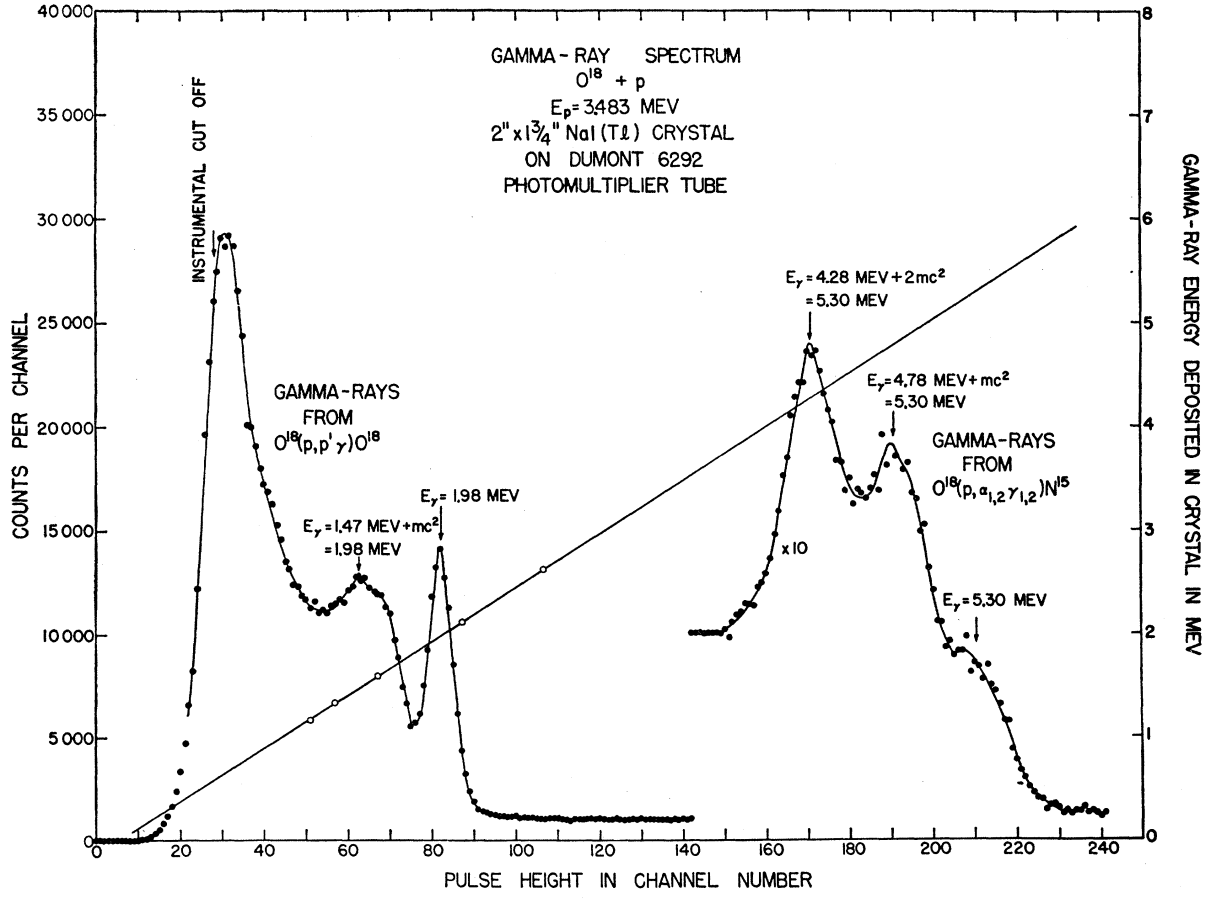

FIG. 7. Gamma-ray spectrum at E_p=3483-kev resonance. Open circles are energy-calibration points.

TABLE II. Variation of elastic scattering cross-section for $O^{18}+p$ with increasing energy.

	Backward angle	90°
s wave	dip, then rise	dip, then small rise
d wave	rise, then dip	dip, then small rise
g wave	rise, then dip	rise, then dip

to zero are expected to be negligible from their hard sphere scattering value, $\psi_{pl}=-\tan^{-1}[F_l(ka)/G_l(ka)]$, for the energy range under consideration. $F_l(ka)$ and $G_l(ka)$ are the regular and irregular Coulomb wave functions, respectively, and a is the nuclear radius (set equal to 5.3 fermis). The s-wave potential phase shift, however, was used as a fitting parameter with a view to taking some account of distant levels (of the same spin and parity).[20] Happily the values used were close to those expected from hard sphere scattering and showed a smooth change with energy.

From the above expression it can be seen that the presence of a pronounced dip in the elastic scattering cross section at 90° in the center-of-mass system can occur only if there is destructive interference of the Coulomb scattering amplitude and the nuclear scattering amplitude. Since the coherent nuclear scattering amplitude is proportional to $P_l(\cos\theta)$, such a resonance must be caused by an even l value. The resonance at 844 kev is an example. For $O^{18}+p$ in the energy region from about 1-Mev to 2-Mev proton energy, the variation of the elastic scattering cross section with increasing energy for s-, d-, and g-wave resonances is characterized in Table II. This qualitative behavior is restricted to the immediate vicinity of the resonance.

An upper limit on the value of l responsible for a resonance can be found from the total reaction cross section at resonance—$(2\pi/k^2)(2J+1)a_{pl}^{\pm}(1-a_{pl}^{\pm})$. The fractional proton partial width, $a_{pl}^{\pm}$, is given by the expression—$(2kP/\Gamma)(3\hbar^2/2\mu a)\theta_{pl}^2$. μ is the proton reduced mass, P is the penetrability {taken to be $[F_l^2(ka)+G_l^2(ka)]^{-1}$}, and θ_{pl}^2 is the dimensionless reduced width. The calculated value of $a_{pl}^{\pm}$, assuming the reduced width has a value equal to the Wigner limit of one,[21] will decrease extremely rapidly as l is increased. This results in an upper limit for l in cases when the total reaction cross section can be obtained.

Analysis for $p\alpha_0$ Reactions

The (p,α_0) cross section takes the form:

$$d\sigma/d\Omega=(A_{l_1}^{J_1}/k)^2[F_{J_1}(\theta)+r^2F_{J_2}(\theta)+2r\cos\Phi I_{J_1J_2l_1l_2}(\theta)],$$

for a level of spin J_2 interfering with a level of spin J_1 in the compound nucleus and a target with spin zero. This may be derived from the general expression given for the differential cross section in the one level (of same spin and parity) approximation by Lane and Thomas.[21] This general expression is also the starting point for the derivation of the elastic scattering differential cross section. The notation is the same as that used for the elastic scattering, with the abbreviations:

$$A_l^J=(a_{pl}^{\pm})^{\frac{1}{2}}(a_{\alpha,\,2J-l}^{\pm})^{\frac{1}{2}}\sin\delta_l^J,$$

$$r=A_{l_2}^{J_2}/A_{l_1}^{J_1},$$

$$\Phi=\omega_{pl_1}+\psi_{pl_1}+\omega_{\alpha,2J_1-l_1}+\psi_{\alpha,2J_1-l_1}+\delta_{l_1}^{J_1}-\omega_{pl_2}-\psi_{pl_2}-\omega_{\alpha,2J_2-l_2}-\psi_{\alpha,2J_2-l_2}-\delta_{l_2}^{J_2}.$$

The exact positions and widths of the interfering levels determine the values of δ_l^J, where J is put in place of $\pm$ to bring out the dependence of the α_0 angular distribution on J rather than l. In the present case, r and Φ were taken as fitting parameters; however, A^2 becomes simply $a_p(1-a_p)$ at resonance. The functions $F_J(\theta)$ give the angular distributions which would occur if each level were present alone and $I_{J_1J_2l_1l_2}(\theta)$ gives the interference contribution:

$$F_J(\theta)=(J+\tfrac{1}{2})^2[P_{J-\frac{1}{2}}(\cos\theta)]^2+\sin^2\theta[P_{J-\frac{1}{2}}'(\cos\theta)]^2,$$

$$I_{J_1J_2l_1l_2}(\theta)=(J_1+\tfrac{1}{2})(J_2+\tfrac{1}{2})P_{J_1\pm\frac{1}{2}}(\cos\theta)P_{J_2\pm\frac{1}{2}}(\cos\theta)+(-1)^{(J_1-l_1+J_2-l_2+1)}\sin^2\theta P_{J_1\pm\frac{1}{2}}'(\cos\theta)\times P_{J_2\pm\frac{1}{2}}'(\cos\theta).$$

The choice of sign in the order of the Legendre polynomial in the interference term depends on the relative values of J_1, J_2, l_1, l_2. The negative sign is used in all four positions except when $J_1>l_1$ while $J_2<l_2$ or when $J_1<l_1$ while $J_2>l_2$. In these cases the positive sign is used in conjunction with whichever spin J is the lesser, or, if $J_1=J_2$, in conjunction with either J_1 or J_2.

The interference term depends on the relative parities of the two levels, and does not depend on the assignment of parity to one of them. This may be proven by expanding the products of Legendre polynomials and their derivatives in the general expression into series of Legendre polynomials and using the known formulas[22] for the Clebsch-Gordon coefficients obtained. Also, of course, the angular distribution for each of the two levels separately depends only on J, not on l. The proton elastic scattering is needed to determine the absolute parity of the levels. Special cases of the above angular distribution have been calculated previously.[6] A particularly simple example is that of two levels of spin $\frac{1}{2}$ and opposite parity:

$$d\sigma/d\Omega=(A/k)^2(1+r^2+2r\cos\Phi\cos\theta).$$

This case is clearly applicable to the 844-kev resonance.

The expression for the (p,α_0) cross section can easily be extended to cases involving interference of any number of levels (of different spin or parity). For three

[20] R. F. Christy, Physica **22**, 1009 (1956); E. U. Baranger, Phys. Rev. **99**, 145 (1955).

[21] T. Teichmann and E. P. Wigner, Phys. Rev. **87**, 123 (1952); A. M. Lane and R. G. Thomas, Revs. Modern Phys. **30**, 257 (1958).

[22] M. E. Rose, *Elementary Theory of Angular Momentum* (J. Wiley & Sons, New York, 1957), p. 47.

interfering levels one must add a term (inside the bracket) giving the separate contribution of the additional level, $(r')^2F_{J_3}(\theta)$, and two terms giving the interference between this third level and the other two levels, $2r'\cos\Phi' I_{J_1J_3l_1l_3}(\theta)$ and $2rr'\cos(\Phi'-\Phi)I_{J_2J_3l_2l_3}(\theta)$.

SPIN AND PARITY ASSIGNMENT OF LEVELS

8.763-kev Level ($E_p=844$ kev)

From the study of the angular distribution of the (p,α_0) reaction, Cohen[6] assigned spin $\frac{1}{2}$ to this level but was unable to make a parity assignment. However, he indicated that the parity of this level has to be opposite to that of a broad underlying spin $\frac{1}{2}$ level in the 700- to 800-kev region (the level is so broad that its position cannot be fixed with any accuracy). The same conclusion is drawn from the (p,α_0) angular distribution in Fig. 5.

Since there is a pronounced dip in the elastic scattering cross section at 90° in the center-of-mass system at the 844-kev resonance, this resonance cannot be due to p-wave protons. Consequently, the level must have even parity. The underlying level must then have odd parity.

Figure 8 shows the calculated curve fitted to the experimental points for the elastic scattering at the 844-kev resonance with the parameters: $a_{p0}{}^{+}=0.62$, $\varphi_{p0}=-10°$, $\Gamma=52$ kev. The curves fitted to the angular

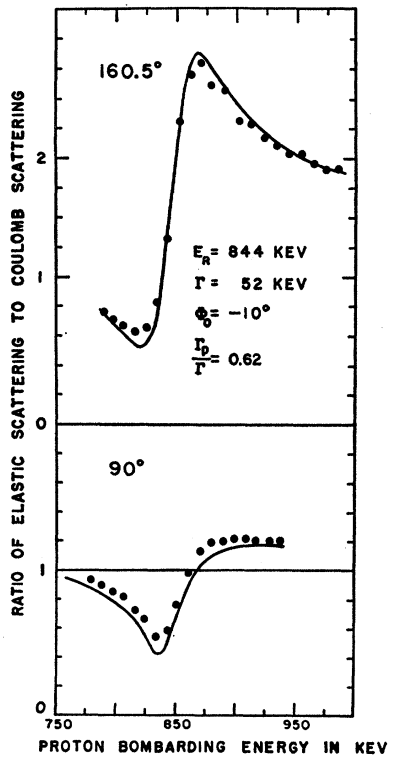

FIG. 8. Calculated curves fitted to elastic scattering data at 844-kev resonance.

TABLE III. Level characteristics.

Resonance (kev)	Excitation (Mev)	l value	Spin and parity	Width (kev)	$a_p{}^{\pm}$	$\theta_p{}^2$	$\theta_\alpha{}^2$
844	8.763	0	$\frac{1}{2}+$	52	0.62	0.09	0.007
1736	9.609	1	$\frac{3}{2}-$				
1765	9.636	2	$\frac{3}{2}+$				
2007	9.865	0	$\frac{1}{2}+$	32	0.34	0.003	0.006

distributions shown in Fig. 5 for the 844-kev resonance were calculated using the same parameters and the following parameters specifying the interference: $r=0.11$, $\Phi=0°$. The elastic scattering is not sensitive to the latter parameters. The level characteristics are listed in Table III.

9.609-Mev Level ($E_p=1736$-kev Resonance) and 9.636-Mev Level ($E_p=1765$-kev Resonance)

Looking at the angular distribution of the (p,α_0) reaction in Fig. 5, it is seen that the distribution at 1765 kev is nearly symmetric about 90° whereas that at 1736 kev is quite asymmetric. This implies that the 1765-kev resonance has little interference from that at 1736 kev but the latter has considerable interference from the former. The two levels, of course, have opposite parity.

The measured width of the 1765-kev resonance, 8 kev, is only slightly greater than the energy resolution; consequently, corrections[23] must be applied to obtain the true size of the (p,α_0) peak which must be considerably greater than observed. These corrections are sufficiently uncertain in the present case that no accurate values for proton partial width could be obtained. However, it is still correct to say that the l values of more than 4 are impossible.

The narrowness of the 1765-kev anomaly in the elastic scattering makes an accurate fitting and the determination of the proton partial width impossible. However, conclusions can still be drawn from the qualitative behavior of the cross section as a function of energy. The pronounced dip in the cross section at 90° indicates that the 1765-kev resonance must be due to an even l value. From Table II, the resonance arises from d-wave excitation. An s-wave potential phase shift of $-15°$ gives good agreement with the observed cross section away from the resonance.

Of the two spin choices, the spin $\frac{3}{2}+$ gives a (p,α_0) angular distribution in reasonable agreement with observation but the spin $\frac{5}{2}+$ does not. The calculated curve is plotted in Fig. 5 but, in this case, the curve is normalized at one point. The normalization is necessary because the yield is reduced by the lack of adequate energy resolution although the relative yield at different angles is unchanged. The comparison with the calculated curve is better made with the curve obtained by

[23] F. B. Hagedorn, F. S. Mozer, T. S. Webb, W. A. Fowler, and C. C. Lauritsen, Phys. Rev. **105**, 219 (1957).

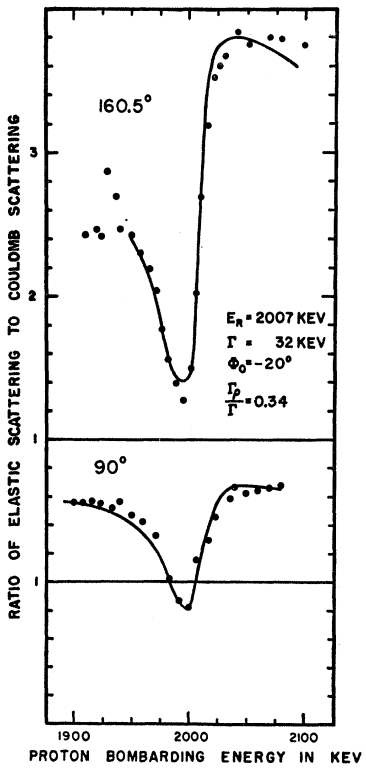

FIG. 9. Calculated curves fitted to elastic scattering at 2007-kev resonance.

averaging measurements taken at angles θ and $180-\theta$ since this eliminates the interference contribution from interfering levels of opposite parity. Such a comparison shows that there must be interference present from levels of even parity as well as that from the level at 1736 kev. Without the absolute value of the (p,α_0) cross section and the true anomaly size, no further analysis in terms of the strengths of these interferences can be made.

The spin of the level at 1736 kev was obtained by comparing the experimental (p,α_0) angular distribution with ones calculated taking into account interference between a $\frac{3}{2}^+$ level at 1765 kev and a level at 1736 kev with spin $\frac{1}{2}^-$, $\frac{3}{2}^-$, $\frac{5}{2}^-$, and $\frac{7}{2}^-$. For these cases the interference term has $\cos\theta$ as a factor so the value of r^2 was taken straight off the energy dependence of the (p,α_0) cross section in Fig. 3. Only the $\frac{3}{2}^-$ choice corresponded to the observed angular distribution. The fitting parameters were $r=0.45$ and $\Phi=180°$. The normalized curve is drawn through the points in Fig. 5. A comparison with the folded curve as at 1765 kev shows that there are interference effects from odd parity levels present. These are small in comparison with that from the level at 1765 kev, however. Because of the strong interference and the smallness of the anomaly, no attempt was made at more detailed fitting.

9.865-Mev Level ($E_p=2007$ kev)

The measured width of 32 kev and the total reaction cross section of 300 mb serve to limit the l value of this resonance to 4 or less. The pronounced dip in the elastic scattering cross section at 90° indicates an even value for l and Table II shows that this must be an s-wave resonance.

In Fig. 9 the curve is calculated for $l=0$ with $a_{p0}{}^+=0.34$, $\Gamma=32$ kev, $\varphi_{p0}=-20°$. This curve and the calculated elastic scattering angular distribution are not sensitive to the interference of the neighboring levels as is the case for the $p\alpha_0$ angular distribution. The latter indicates interference coming from two neighboring levels of spins $\frac{3}{2}^+$ and $\frac{1}{2}^-$. No single neighboring level could give the observed (p,α_0) angular distribution. The fitting parameters used in Fig. 8 are $r=0.115$, $\Phi=0°$ for the $\frac{3}{2}^+$ level, and $r'=0.17$, $\Phi=0°$ for the $\frac{1}{2}^-$ level. The contributions to the angular distribution are almost wholly from the interference of these two levels with the $\frac{1}{2}^+$ level. Both the (p,p) and (p,α_0) angular distributions were corrected for the off-resonance measurement. The main characteristics of the 2007-kev level can be explained only by assuming $l=0$. The level characteristics are given in Table III.